Available online at www.sciencedirect.com
ScienceDirect
Journal of Bionic Engineering 12 (2015) 527–538

Type Synthesis for Bionic Quadruped Walking Robots

Jun He, Feng Gao

State Key Laboratory of Mechanical System and Vibration, *Shanghai Jiao Tong University*, *Shanghai* 200240, *China*

Abstract

Regarding walking robots, biomimetic design has attracted a great deal of attention. Currently, studies have focused mainly on performance analysis and the design of some specific biomimetic walking robots. However, the systematic type synthesis of bionic quadruped robots has seldom been studied. In this paper, a new approach to type synthesis for quadruped walking robots is proposed based on the generalized function ($\boldsymbol{G_F}$) set theory. The current types of typical walking robots are analyzed using the $\boldsymbol{G_F}$ set theory. The research status and existing problems are investigated. The skeletal systems of quadruped mammals are analyzed. The motion characteristics of all joints of quadruped mammals are denoted by $\boldsymbol{G_F}$ sets. A process of conversion from biological types to serial, parallel and hybrid types is proposed. Limb types in serial, parallel and hybrid topology are synthesized. Finally the quadruped robots with serial, parallel and hybrid topology are produced. Two of these types have been successfully used for the design of walking rescue robots that is suitable for responding to nuclear accidents.

Keywords: type synthesis, bionic design, quadruped robot, parallel mechanism, $\boldsymbol{G_F}$ set

doi: 10.1016/S1672-6529(14)60143-8

Nomenclatures

P	Translation pair
R	Rotation pair
U	Universal pair
S	Spherical pair
$^{\wedge}U$	Rotation-translation universal pair
$U^{\wedge}$	Translation-rotation universal pair
^{P}U	Pure-planar-translation universal pair
U^{P}	Pure-translation-planar universal pair
P^{R}	Parallelogram prismatic pair
U^{*}	Pure-translation universal pair

1 Introduction

Multi-legged robots have better mobility in uneven terrain than wheeled or tracked vehicles because they can use discrete footholds for each step. In dangerous and dirty environments that wheeled and tracked vehicles cannot reach, multi-legged robots can replace humans and carry out special tasks such as disaster response. For example, the walking robot SCHAFT was designed to drive cars, open doors, climb industrial ladders, and remove debris blocking entryways in nuclear power plant for disaster relief[1]. Legged robots may also carry military supplies in the future. The quadruped robot BigDog from Boston Dynamics has been tested for military missions[2–3].

The mechanism type is a kinematic arrangement for a given motion pattern. The type synthesis is defined as the process of finding all possible types of robotic mechanisms which can generate a specified motion pattern of the end-effector[4]. Type synthesis is an important issue for robotic mechanisms. The type of mechanism affects the general performance of a walking robot in such respects as mobility, workspace, and singularity. There are many ways of type synthesis that involve various mathematical tools, such as screw theory, Lie group, and differential manifolds. Kong *et al*.[4] were the first to carry out type synthesis of Parallel Mechanisms (PMs) with multiple operation modes using the virtual-chain approach. Kong *et al*. presented a method for the type synthesis of PMs based on the screw theory, which was used for type synthesis of 3-DOF translational PMs[5] and 3T1R 4-DOF PMs[6]. Kong *et al*. also proposed a method for the type synthesis of spherical PMs[7]. They also first discover the phenomenon of dependent joint groups in the spherical parallel kinematic chain. Huang *et al*. proposed general methodology for

Corresponding author: Feng Gao
E-mail: fengg@sjtu.edu.cn

type synthesis of symmetrical lower-mobility PMs using the reciprocal screw theory[8]. Screw theory can be used to analyze the instantaneous motions of mechanisms[9]. However, it cannot indicate the effect of the order of the rotations and the translations. Full-cycle mobility of all synthesized mechanisms must be checked. Gogu presented a new approach to structural synthesis of fully-isotropic translational parallel robotic manipulators based on the theory of linear transformations[10]. Yang *et al*. performed a systematic study of the type synthesis of 3T1R PMs using the units of a single-opened-chain[11]. Xie *et al*. presented a type synthesis method based on Grassmann line geometry and the atlas method to deal with the design of the 4-DOF PMs[12]. This method was able to reduce the complexity of the PMs' type synthesis. Fan *et al*. systematically synthesized PMs with 2T2R 4-DOFs based on the integration of configuration evolution and Lie group theory[13]. The Lie groups and differential manifolds provide precise mathematical descriptions of the motion characteristics of kinematic pairs and chains[14,15]. However, Lie sub-groups cannot be used when the end-effector has two rotational DOFs or the rotational DOFs are larger than the translational DOFs[16]. Recently, Gao *et al*. proposed the $\boldsymbol{G_F}$ set theory for the type synthesis of robotic mechanisms, by which many novel mechanisms can be synthesized[17,18]. The $\boldsymbol{G_F}$ set is used to express the kinematic characteristics of the end-effectors, which are defined as follows:

$$\boldsymbol{G_F} = (P_a \;\; P_b \;\; P_c;\; R_\alpha \;\; R_\beta \;\; R_\gamma), \tag{1}$$

Here, (P_a, P_b, P_c) and (R_α, R_β, R_γ) are the translational and rotational characteristics of the end-effectors. The $\boldsymbol{G_F}$ sets can be grouped into three categories: the first class of $\boldsymbol{G_F}$ sets with completeness of rotation characteristics, the second class of $\boldsymbol{G_F}$ sets with non-completeness of rotation characteristics and the third class of $\boldsymbol{G_F}$ sets with partial completeness of rotation characteristics[19,20].The $\boldsymbol{G_F}$ sets can be also used for the analysis of kinematic characteristics of robotic mechanisms. Yang *et al*. and Miao *et al*. both studied the state classifications for human hands and the lower extremity exoskeleton via the $\boldsymbol{G_F}$ set theory[21,22]. The $\boldsymbol{G_F}$ sets were used to indicate the kinematic characteristics of the end effectors in different states.

Each specified quadruped mammal has a solely biological configuration. However, this biological configuration may be not suitable for the design of quadruped robots with specific purposes. It was necessary to find as many configurations of walking robots as possible. A biological configuration can produce a very large number of kinematic arrangements with serial, parallel, or hybrid topology for a given motion pattern. For this reason, a systematic approach is needed to determine all types of configurations of walking robots, thereby allowing the development of the most promising designs. The type synthesis of multi-legged robot is more complicated than that of serial or parallel robotic mechanisms. The topological state of the walking robot changes when the robot walks at different gaits[23]. The DOFs of robot bodies in crawling gait can be different from those in trotting gaits. The uncertainty of topological states increases the difficulty of the type synthesis of multi-legged robots. Table 1 shows the types of mechanisms of existing typical walking robots[2,3,24–37]. "*R*" "*P*" and "*U*" denote the rotary, prismatic, and universal joints, respectively. Underlining denotes the active joint. The subscripts "*r*" "*p*" and "*y*" denote the roll, pitch, and yaw motion characteristics, respectively. There are three typical types of contact between the foot of a walking robot and the ground: point contact, line contact, and fixed contact. These are here regarded as the spherical, revolute, and fixed joints, respectively. The motion characteristics of the legs and bodies are all expressed using $\boldsymbol{G_F}$ sets. Most of the present leg configurations are connected in serial, which is beneficial to dynamic control. Legs with parallel topology are stiffer and have greater payload capacity than their serial counterparts. In some special environments, like those with nuclear radiation, the electric devices of the actuator have to be shielded. For a parallel leg, the actuators can be centrally mounted on a single base platform. The electric devices of actuators can be protected from damage easily. In the meantime, the centralization of mass reduces the robot's overall moment of inertia, which is beneficial to the walking of legged robots. There are few multi-legged robots with waist joints. Only the Asguard robot has a rotary waist joint[25]. The introduction of a waist joint makes control more difficult, but the waist joint can improve the dexterity of a multi-legged robot and increase its stride and running speed just like it does in living animals.

Though walking robots have attracted a great deal of attention, researchers have mainly focus on the

Table 1 Mechanisms of existing walking robots

Name	Leg			Foot	Body
	DOFs	Configuration	$\boldsymbol{G_F}$ sets	Contact	$\boldsymbol{G_F}$ sets
RHex[24]	1	$\underline{R}_p$	$\boldsymbol{G}_{Fi}^{II}(R_{\alpha i},0,0,0,0,0)$	R_p	$\boldsymbol{G}_{F}^{II}(R_{\alpha},P_a,0,0,0,0)$
Asguard[25]	1	$\underline{R}_p$	$\boldsymbol{G}_{Fi}^{II}(R_{\alpha i},0,0,0,0,0)$	R_p	$\boldsymbol{G}_{Ffb}^{II}(R_{\alpha},R_{\beta},P_a,0,0,0)$ $\boldsymbol{G}_{Fbb}^{II}(R_{\alpha},R_{\beta},P_a,0,0,0)$
Whegs-I[26]	1	$\underline{R}_p$	$\boldsymbol{G}_{Fi}^{II}(R_{\alpha i},0,0,0,0,0)$	R_p	$\boldsymbol{G}_{F}^{II}(R_{\alpha},P_a,0,0,0,0)$
Whegs-II[26]	1	$\underline{R}_p$	$\boldsymbol{G}_{Fi}^{II}(R_{\alpha i},0,0,0,0,0)$	R_p	$\boldsymbol{G}_{Ffb}^{II}(R_{\alpha},P_a,P_b,0,0,0)$ $\boldsymbol{G}_{Fbb}^{II}(R_{\alpha},P_a,P_b,0,0,0)$
Sprawlita[27]	2	$\underline{R}_pP$	$\boldsymbol{G}_{Fi}^{II}(R_{\alpha i},P_{ai},0,0,0,0)$	S	$\boldsymbol{G}_{F}^{III}(R_{\alpha},R_{\beta},R_{\gamma},P_a,P_b,0)$
Scout II[28]	2	$\underline{R}_pP$	$\boldsymbol{G}_{Fi}^{II}(R_{\alpha i},P_{ai},0,0,0,0)$	S	$\boldsymbol{G}_{F}^{III}(R_{\alpha},R_{\beta},R_{\gamma},P_a,P_b,0)$
Quadruped[29]	3	$\underline{U}\,\underline{P}$	$\boldsymbol{G}_{Fi}^{II}(R_{\alpha i},R_{\beta i},P_{ai},0,0,0)$	S	$\boldsymbol{G}_{F}^{III}(R_{\alpha},R_{\beta},R_{\gamma},P_a,P_b,0)$
SILO6[30]	3	$\underline{R}_y\underline{R}_p\underline{R}_p$	$\boldsymbol{G}_{Fi}^{II}(R_{\alpha i},R_{\beta i},P_{ai},0,0,0)$	S	$\boldsymbol{G}_{F}^{III}(R_{\alpha},R_{\beta},R_{\gamma},P_a,P_b,0)$
ASV[31]	4	$\underline{R}_i\underline{R}_p\underline{R}_p\underline{R}_p$	$\boldsymbol{G}_{Fi}^{II}(R_{\alpha i},R_{\beta i},P_{ai},P_{bi},0,0)$	Fixed	$\boldsymbol{G}_{F}^{II}(R_{\alpha},R_{\beta},P_a,0,0,0)$
HyQ[32]	4	$\underline{R}_y\underline{R}_p\underline{R}_pP$	$\boldsymbol{G}_{Fi}^{II}(R_{\alpha i},R_{\beta i},P_{ai},P_{bi},0,0)$	S	$\boldsymbol{G}_{F}^{III}(R_{\alpha},R_{\beta},R_{\gamma},P_a,P_b,0)$
BigDog2005[2]	4	$\underline{R}_y\underline{R}_p\underline{R}_pP$	$\boldsymbol{G}_{Fi}^{II}(R_{\alpha i},R_{\beta i},P_{ai},P_{bi},0,0)$	R_p	$\boldsymbol{G}_{F}^{II}(R_{\alpha},R_{\beta},P_a,P_b,0,0)$
BigDog2008[3]	5	$\underline{R}_y\underline{R}_p\underline{R}_p\underline{R}_pP$	$\boldsymbol{G}_{Fi}^{II}(R_{\alpha i},R_{\beta i},P_{ai},P_{bi},0,0)$	R_p	$\boldsymbol{G}_{F}^{II}(R_{\alpha},R_{\beta},P_a,P_b,0,0)$
SILO4[33]	6	$\underline{R}_y\underline{R}_p\underline{R}_pS$	$\boldsymbol{G}_{Fi}^{I}(P_{ai},P_{bi},P_{ci},R_{\alpha i},R_{\beta i},R_{\gamma i})$	Fixed	$\boldsymbol{G}_{F}^{I}(P_a,P_b,P_c,R_{\alpha},R_{\beta},R_{\gamma})$
Comet-IV[34]	6	$\underline{R}_y\underline{R}_p\underline{R}_p\underline{R}_pU$	$\boldsymbol{G}_{Fi}^{I}(P_{ai},P_{bi},P_{ci},R_{\alpha i},R_{\beta i},R_{\gamma i})$	Fixed	$\boldsymbol{G}_{F}^{I}(P_a,P_b,P_c,R_{\alpha},R_{\beta},R_{\gamma})$
Baby elephant[35,36]	6	$\underline{R}_y(\underline{R}_p\underline{P})\,S$	$\boldsymbol{G}_{Fi}^{I}(P_{ai},P_{bi},P_{ci},R_{\alpha i},R_{\beta i},R_{\gamma i})$	Fixed	$\boldsymbol{G}_{F}^{I}(P_a,P_b,P_c,R_{\alpha},R_{\beta},R_{\gamma})$
Octopus[37]	6	$(U\underline{P}\&2\text{-}U\underline{P}S)S$	$\boldsymbol{G}_{Fi}^{I}(P_{ai},P_{bi},P_{ci},R_{\alpha i},R_{\beta i},R_{\gamma i})$	Fixed	$\boldsymbol{G}_{F}^{I}(P_a,P_b,P_c,R_{\alpha},R_{\beta},R_{\gamma})$

performance analysis and on the design of specific quadruped robots[38,39]. The type synthesis of multi-legged robots has rarely been studied. Type synthesis of legged robots is very important to the realization of the function. For instance, legged robots suitable for work in nuclear disaster sites must be easy to be protected from nuclear radiation. However, the electronic devices in each actuator are installed separately for serial legs. It would be very valuable to design a leg configuration for which the electronic devices of all actuators can be assembled on the body. This study firstly analyzed the existing types of typical walking robots using the $\boldsymbol{G_F}$ set theory. The research status and existing problems with existing types of walking robots were investigated. The skeletal mechanisms of quadruped mammals were studied. The motion characteristics of all joints of quadruped mammals are here denoted by the $\boldsymbol{G_F}$ sets. Then the process of type synthesis from biological types to serial, parallel, and hybrid types is presented. Using the type synthesis method of $\boldsymbol{G_F}$ sets, limb types with serial, parallel, and hybrid topology are synthesized. Finally, the type synthesis of quadruped robots is carried out based on the biological types of quadruped mammals and the types of limbs.

2 Biological mechanisms of quadruped mammals

It is clear that even the most advanced multi-legged robots perform much more poorly than their biological counterparts. Animal locomotion is versatile, agile, energy-efficient, and elegant. The design of almost all multi-legged robots was inspired by biological mechanisms. The skeletal system of the quadruped mammal generally includes the appendicular skeleton and the axial skeleton. The former contains the bones of the limbs and limb girdles. The latter includes the skull, hyoid apparatus, vertebral column, ribs, and sternum. For example, the skeletal system of a dog is introduced, as shown in Fig. 1[40]. The canine skeletal system has three main parts, *i.e*. the axial skeleton (bones of the head, trunk, and tail), the bones of the thoracic limbs (bones of the forelimbs), and the bones of the pelvic limbs (bones of the hind limbs).

In the anatomy of domestic animals, the motion characteristics of each joint can be determined as follows[41]. The first and second cervical vertebrae are called the atlas and axis, respectively (Fig. 1). The atlas supports the head. It articulates with the occipital

condyles, which forms the atlanto-occipital joint, allowing the head to nod in a "yes" motion, *i.e*. flexion and extension. The axis contains a large, ridge-like spinous process and the dens, a peglike cranial process forming a pivot articulation with the atlas[41]. This allows the head to turn side to side in a "no" motion. The shoulder joint is a ball-and-socket type synovial joint. The carpal joint consists of the antebrachiocarpal, middle carpal, and carpometacarpal joints[41]. These can be regarded as hinged synovial joints (Fig. 2a). The hip joint is also a ball-and-socket synovial joint between the head of the femur and the acetabulum of the hip bone. It is a freely movable joint allowing universal movement, *i.e*. flexion, extension, abduction, adduction, lateral rotation, and circumduction. The knee (*i.e*. the stifle joint) is a compound joint involving the femur, patella, and tibia[41]. It is a hinge synovial joint, allowing flexion and extension with little rotation. The tarsus is also a compound hinge synovial joint. It allows only flexion and extension (Fig. 2b). Table 2 shows the motion characteristics of joints of quadruped mammals and their equivalent kinematic pairs based on $\boldsymbol{G_F}$ sets.

3 Type synthesis of quadruped robots

3.1 Limb types with serial topology

There are two methods by which the kinematic limbs of walking robots can be designed. The first method involves using composite kinematic pairs to replace the combination of simple pairs. Gao *et al*. presented six composite pairs, including the rotation/translation universal pair $\hat{}U$ and $U\hat{}$, the pure-planar-translation universal pair ${}^{P}U$ and U^{P}, the parallelogram prismatic pair P^{R}, and the pure-translation universal pair U^{*}[17]. The second involves changing the location of the revolute joint using the theorem of the rotating axis movement in the 2D plane or the 3D space[17]. In addition, the parallel revolute pairs are used to create the derivative translational characteristics. These substitutions between kinematic pairs can be written as follows:

$$R_i \bigcup R_j = U_{i+j} \quad (i, j = r, p, y;\ i \neq j), \tag{2}$$

$$R_r \bigcup R_p \bigcup R_y = S_{r+p+y}, \tag{3}$$

$$P^R = P_i, \quad i = r, p, y, \tag{4}$$

$$P^R \bigcup R_j = U\hat{} \text{ or } R_j \bigcup P^R = \hat{}U, \quad R_j \in P^R, \tag{5}$$

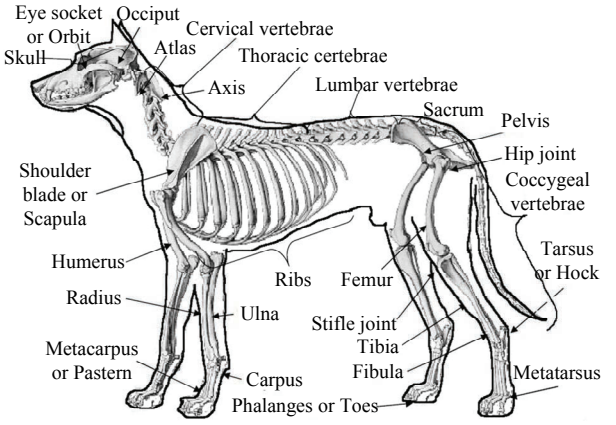

Fig. 1 Skeletal system of a dog[40].

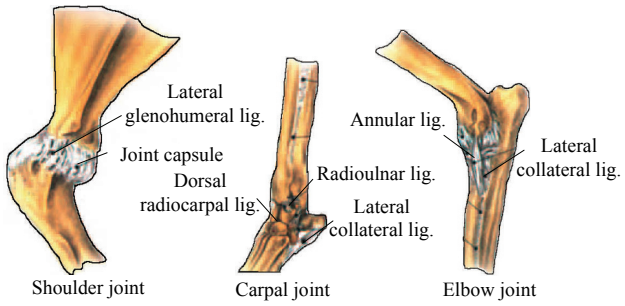

(a) Thoracic limb

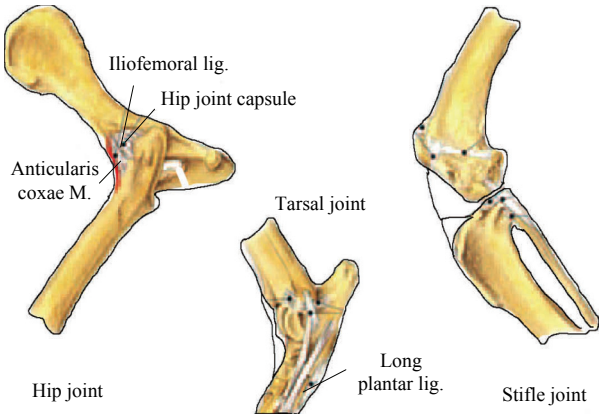

(b) Pelvic limb

Fig. 2 Joints of the thoracic and plevic limb[41].

$$P^R \bigcup P_j = U^P \text{ or } P_j \bigcup P^R = {}^{P}U, \quad P_j \in P^R, \tag{6}$$

$$R_i \bigcup R_i = R_i \bigcup P, P \perp R_i, j = r, p, y, \tag{7}$$

$$R_i \bigcup R_i \bigcup R_i = R_i \bigcup P_j \bigcup P_k, R_i \perp P_j P_k, i = r, p, y, \tag{8}$$

Here, R, P, U and S denote the revolute, prismatic, universal, and spherical pairs, respectively. The kinematic structure of the biological leg can be denoted by

Table 2 Skeletal systems of quadruped mammals

Part	Joint	Type	Mobility	Equivalent pairs	$\boldsymbol{G}_F$ sets of the end of limbs
Head	Cervical vertebrae	Universal joint hinge 5 ball-and-sockets	Flexion Extension Abduction Adduction Lateral rotation Circumduction	R_r-R_p-R_y	$\boldsymbol{G}_{FN}^{II} = \boldsymbol{G}_{FN}^{II}(R_r, R_p, R_y, 0, 0, 0)$
Trunk	Thoracic and lumbar vertebrae	13, 15 or 18 hinges 6 or 7 universal joints	Flexion Extension Abduction Adduction Lateral rotation Circumduction Translation	S-P_r	$\boldsymbol{G}_{FW}^{II} = \boldsymbol{G}_{FW}^{II}(R_r, R_p, R_y, P_r, 0, 0)$
Thoracic limb	Shoulder joint	Ball-and-socket	Flexion Extension Abduction Adduction Lateral rotation Circumduction	S	$\boldsymbol{G}_{FL}^{III} = \boldsymbol{G}_{F}^{III}(R_r, R_y, P_r, P_y, R_p, 0)$
	Elbow joint	Hinge	Flexion Extension	R_p	
	Carpal joint	Hinge	Flexion Extension	R_p	
Pelvic limb	Hip joint	Ball-and-socket	Flexion Extension Abduction Adduction Lateral rotation Circumduction	S	$\boldsymbol{G}_{FL}^{III} = \boldsymbol{G}_{F}^{III}(R_r, R_y, P_r, P_y, R_p, 0)$
	Stifle joint	Hinge	Flexion Extension	R_p	
	Tarsal joint	Hinge	Flexion Extension	R_p	

S_{r+p+y}-R_p-R_p. Fig. 3 shows the design process of a serial leg's kinematic structure from the biological type. For example, according to Eqs. (4) and (5), the kinematic structure of the biological leg can be changed to R_r-R_y-R_p-R_p-R_p, then to R_r-R_y-R_p-P_r-P_y. Using the theorem of the rotating axis movement, the structure is transformed to R_r-R_y-P_r-R_p-P_y or R_r-R_y-P_r-P_y-R_p. Using the composite kinematic pairs, these two structures are further changed to U_{r+y}-P_r-R_p-P_y, U_{r+y}-P_r-P_y-R_p, R_r-R_y-P^R-R_p-P_y, R_r-R_y-P_r-R_p-P^R, R_r-R_y-P^R-P_y-R_p, R_r-R_y-P_r-P^R-R_p, R_r-$\hat{}U$-R_p-P_y, R_r-R_y-$U\hat{}$-P_y, R_r-R_y-U^P-R_p, and so on. Using a similar method, the serial types of the neck and waist joints can be synthesized (Figs. 4 and 5). Finally, 37 kinds of serial legs, 4 kinds of neck joints, and 28 kinds of waist joints were produced. Fig. 6 shows the examples of these necks, waists and legs, all of which have serial topology.

3.2 Limb types with parallel topology

Legs with parallel topology have several advantages over serial legs. The actuators of this kind of leg mechanism are assembled on the body and there are no electronic devices on any moving parts. This makes them easier to protect. The mass and inertia of moving parts are reduced, which improves the dynamics of the leg. With biological legs, the rotating axis of the pitch motion, *i.e*. R_p, is perpendicular to the 2-D translation plane which is built using the P_r and P_y. According to the theorem of rotating axis movement in a 2-D plane in $\boldsymbol{G}_F$ set theory, no matter where the revolute joints are, the end-effector of the kinematic chain can rotate around the axis which is perpendicular to the 2-D plane on the end-effector. In this way, the pitch motion has the characteristic of "completeness"[19]. The motion characteristics of the ends of biological legs are placed in the third class of $\boldsymbol{G}_F$ sets, as follows:

$$\boldsymbol{G}_{FL}^{III} = \boldsymbol{G}_{F}^{III}(R_r, R_y, P_r, P_y, R_p, 0). \quad (9)$$

Here, $\boldsymbol{G}_{FL}^{III}$ denotes the $\boldsymbol{G}_F$ sets of biological legs. According to Meng's study, there are five decomposition combinations of $\boldsymbol{G}_{FL}^{III}$ [19]. To reduce manufacturing costs, the type complexity[20] must be as low as possible. In general, the more geometric constraints the leg type has, the more difficult the structural design becomes. In this way, decomposition combinations without any geometrical constraints have less type complexity. Any type that has only one kind of limb also has less type

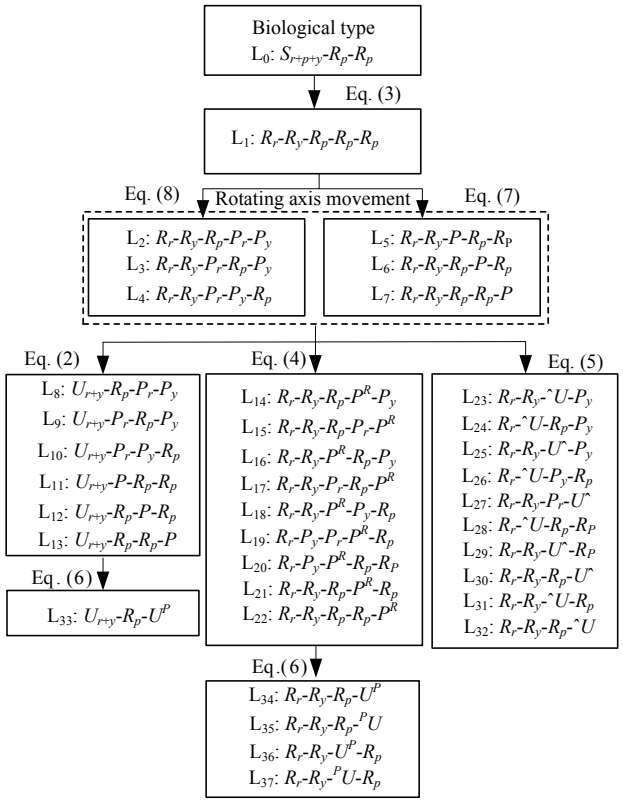

Fig. 3 Configurations of 5-DOF serial limbs.

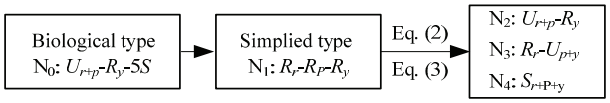

Fig. 4 Configurations of 3-DOF neck joints.

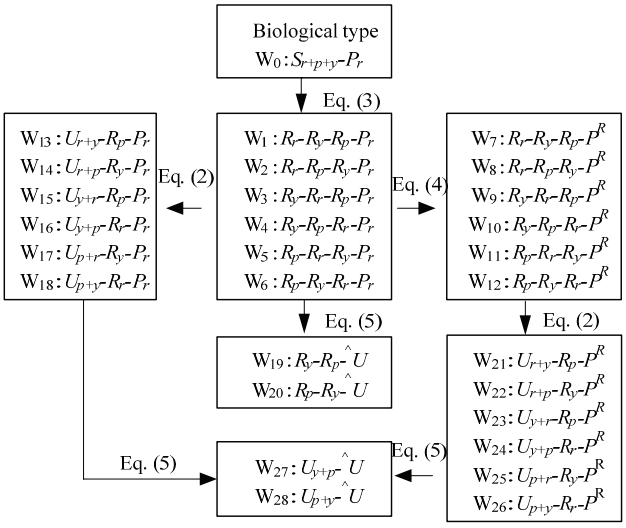

Fig. 5 Configurations of 4-DOF waist joints.

complexity. The decomposition combinations of legs with parallel topology can be denoted as follows:

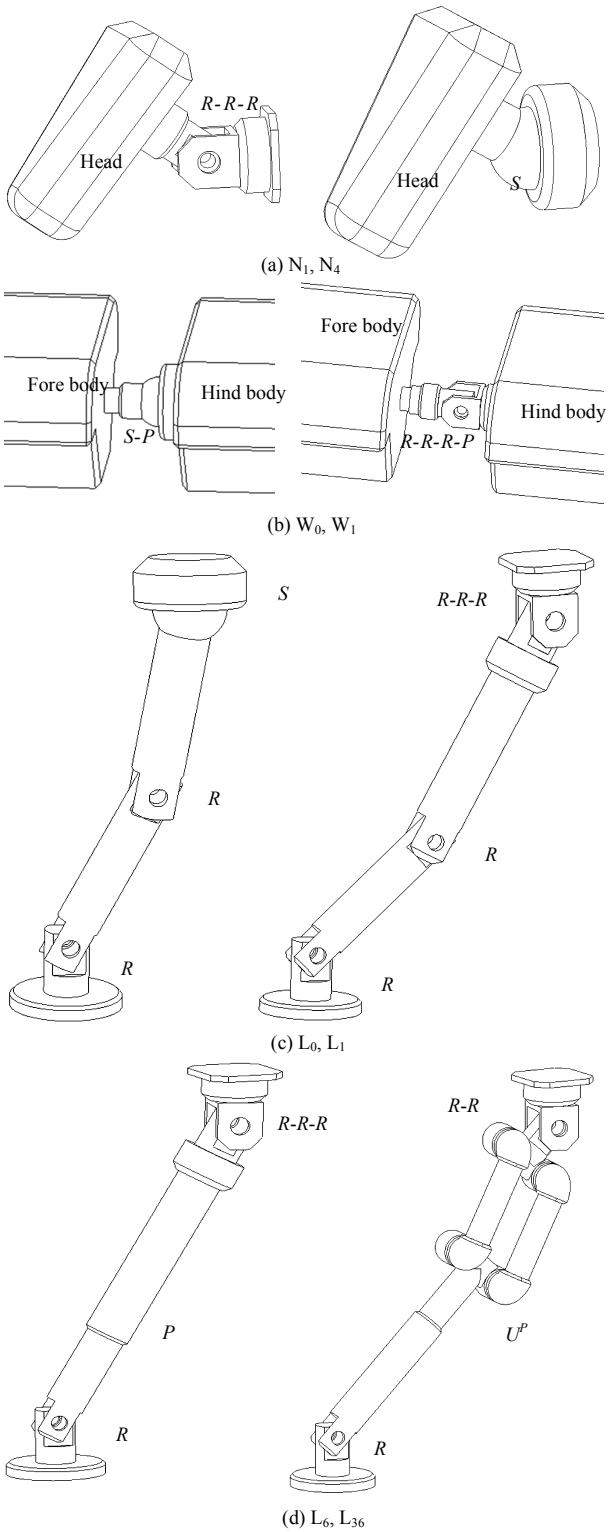

Fig. 6 Structures of necks, waists, and legs with serial topology.

$$\boldsymbol{G}_{FL}^{\mathrm{III}} = \boldsymbol{G}_{FL1}^{\mathrm{III}}\left(R_{\alpha 1}, R_{\beta 1}, P_{a1}, P_{b1}, R_{\gamma 1}, 0\right) \bigcap \left(\bigcap_{i=2}^{5} \boldsymbol{G}_{FLi}^{1}\left(P_{ri}, P_{pi}, P_{yi}, R_{ri}, R_{pi}, R_{yi}\right) \right), \quad (10)$$

$$\boldsymbol{G}_{\boldsymbol{F}\mathrm{L}}^{\mathrm{III}}=\bigcap_{i=1}^{5}\boldsymbol{G}_{\boldsymbol{F}\mathrm{L}i}^{\mathrm{III}}\left(R_{\alpha 1},\,R_{\beta 1},\,P_{a1},\,P_{b1},\,R_{\gamma 1},0\right),\qquad(11)$$

Here, $\boldsymbol{G}_{\boldsymbol{F}\mathrm{L}}^{\mathrm{III}}$ is the $\boldsymbol{G}_{\boldsymbol{F}}$ sets of the first limb which is belong to the third class $\boldsymbol{G}_{\boldsymbol{F}}$ sets. $\boldsymbol{G}_{\boldsymbol{F}\mathrm{L}i}^{\mathrm{I}}$ (i = 2–5) denote $\boldsymbol{G}_{\boldsymbol{F}}$ sets of the others limbs which is belong to the first class $\boldsymbol{G}_{\boldsymbol{F}}$ sets.

The $\boldsymbol{G}_{\boldsymbol{F}}$ sets of the neck and waist joints can be written as follows:

$$\boldsymbol{G}_{\boldsymbol{F}\mathrm{N}}^{\mathrm{II}}=\boldsymbol{G}_{\boldsymbol{F}\mathrm{N}}^{\mathrm{II}}\left(R_r,\,R_p,R_y,\,0,\,0,\,0\right),\qquad(12)$$

$$\boldsymbol{G}_{\boldsymbol{F}\mathrm{W}}^{\mathrm{II}}=\boldsymbol{G}_{\boldsymbol{F}\mathrm{W}}^{\mathrm{II}}\left(R_r,\,R_p,R_y,\,P_r,\,0,\,0\right).\qquad(13)$$

Here, $\boldsymbol{G}_{\boldsymbol{F}\mathrm{N}}^{\mathrm{II}}$ and $\boldsymbol{G}_{\boldsymbol{F}\mathrm{W}}^{\mathrm{II}}$ are the $\boldsymbol{G}_{\boldsymbol{F}}$ sets of the neck and waist joints. The decompositions with the lowest type complexities are obtained as follows:

$$\boldsymbol{G}_{\boldsymbol{F}\mathrm{N}}^{\mathrm{II}}=\boldsymbol{G}_{\boldsymbol{F}\mathrm{N}1}^{\mathrm{II}}\left(R_r,\,R_p,R_y,\,0,\,0,\,0\right)\cap\left(\bigcap_{i=2}^{3}\boldsymbol{G}_{\boldsymbol{F}\mathrm{N}i}^{\mathrm{I}}\left(P_{ri},\,P_{pi},\,P_{yi},\,R_{ri},\,R_{pi},\,R_{yi}\right)\right),\qquad(14)$$

$$\boldsymbol{G}_{\boldsymbol{F}\mathrm{N}}^{\mathrm{II}}=\bigcap_{i=1}^{3}\boldsymbol{G}_{\boldsymbol{F}\mathrm{N}i}^{\mathrm{II}}\left(R_r,\,R_p,R_y,\,0,\,0,\,0\right),\qquad(15)$$

$$\boldsymbol{G}_{\boldsymbol{F}\mathrm{W}}^{\mathrm{II}}=\boldsymbol{G}_{\boldsymbol{F}\mathrm{W}1}^{\mathrm{II}}\left(R_r,\,R_p,R_y,\,P_r,\,0,\,0\right)\cap\left(\bigcap_{i=2}^{4}\boldsymbol{G}_{\boldsymbol{F}\mathrm{W}i}^{\mathrm{I}}\left(P_{ri},\,P_{pi},\,P_{yi},\,R_{ri},\,R_{pi},\,R_{yi}\right)\right),\qquad(16)$$

$$\boldsymbol{G}_{\boldsymbol{F}\mathrm{W}}^{\mathrm{II}}=\bigcap_{i=1}^{4}\boldsymbol{G}_{\boldsymbol{F}\mathrm{W}i}^{\mathrm{II}}\left(R_r,\,R_p,R_y,\,P_r,\,0,\,0\right).\qquad(17)$$

Here, $\boldsymbol{G}_{\boldsymbol{F}\mathrm{N}1}^{\mathrm{II}}$ and $\boldsymbol{G}_{\boldsymbol{F}\mathrm{W}1}^{\mathrm{II}}$ are the $\boldsymbol{G}_{\boldsymbol{F}}$ sets of the first limbs of the neck and waist joints, which are belong to the second class $\boldsymbol{G}_{\boldsymbol{F}}$ sets. $\boldsymbol{G}_{\boldsymbol{F}\mathrm{N}i}^{\mathrm{I}}$ and $\boldsymbol{G}_{\boldsymbol{F}\mathrm{W}i}^{\mathrm{I}}$ (i = 2–5) denote $\boldsymbol{G}_{\boldsymbol{F}}$ sets of the others limbs of the neck and waist joints, respectively. According to the decomposition combinations of $\boldsymbol{G}_{\boldsymbol{F}}$ sets, 12 kinds of leg, neck, and waist types can be produced (Table 3). Fig. 7 shows examples of leg, neck, and waist structures with parallel topology.

3.3 Limb types with hybrid topology

In practice, the leg mechanism of quadruped robots provides the points of contact with the ground in three-dimensional space. A 3-DOF leg configuration can produce the required motion. It is somewhat complicated to adopt the 5-DOF parallel mechanism for the leg design directly. For these reasons, the leg configuration should be a series-parallel and active-passive hybrid kinematic chain. The parallel mechanism is the active component and other mechanisms are passive. To reduce the mass and inertia of the moving parts, the parallel actuation components should be arranged as close to the robot's body as possible. The first three kinematic pairs or the second and third kinematic pairs can be combined; they take a parallel topology when they are connected in a series. Suitable parallel mechanisms with 2-DOFs and 3-DOFs include RR, RP, RRR and RRP configurations. In general, two passive rational axes are necessary to

Table 3 Types of limbs with parallel topology

Part	$\boldsymbol{G}_{\boldsymbol{F}}$ sets of limbs	Example of type	
Leg	$\boldsymbol{G}_{\boldsymbol{F}\mathrm{L}1}^{\mathrm{III}}\left(R_{\alpha 1},\,R_{\beta 1},\,P_{a1},\,P_{b1},\,R_{\gamma 1},0\right)\cap\left(\bigcap_{i=2}^{5}\boldsymbol{G}_{\boldsymbol{F}\mathrm{L}i}^{\mathrm{I}}\left(P_{ri},\,P_{pi},\,P_{yi},\,R_{ri},\,R_{pi},\,R_{yi}\right)\right)$	L_{38}: 1-*SRR*&4-*SPS*; L_{40}: 1-*RRRPR*&4-*SPS*; L_{42}: 1-*URPP*&4-*SRS*; L_{44}: 1-*URU*^{P}&4-*PU***S*; L_{46}: 1-*RRU*^{P}R&4-*PPPS*;	L_{39}: 1-*RRRRR*&4-*PSS*; L_{41}: 1-*RRPRR*&4-*PUS*; L_{43}: 1-*RRRPRP*&4-*RSS*; L_{45}: 1-*RR*$\hat{}$*UP*&4-*U***PS*; L_{47}: 1-*RRU*$\hat{}$*P*&4-$P_aP_aP_aS$
	$\bigcap_{i=1}^{5}\boldsymbol{G}_{\boldsymbol{F}\mathrm{L}i}^{\mathrm{III}}\left(R_{\alpha 1},\,R_{\beta 1},\,P_{a1},\,P_{b1},\,R_{\gamma 1},0\right)$	L_{48}: 5-*SRR*	L_{49}: 5- *URPP*
Neck	$\boldsymbol{G}_{\boldsymbol{F}\mathrm{N}1}^{\mathrm{II}}\left(R_r,\,R_p,R_y,\,0,\,0,\,0\right)\cap\left(\bigcap_{i=2}^{3}\boldsymbol{G}_{\boldsymbol{F}\mathrm{N}i}^{\mathrm{I}}\left(P_{ri},\,P_{pi},\,P_{yi},\,R_{ri},\,R_{pi},\,R_{yi}\right)\right)$	N_5: 1-*RRR*&2-*SPS*; N_7: 1-*UR*&2-*UPS*; N_9: 1-*RU*&2-*SRS*; N_{11}: 1-*S*&2-*PU***S*;	N_6: 1-*RRR*&2-*PSS*; N_8: 1-*UR*&2-*PUS*; N_{10}: 1-*RU*&2-*RSS*; N_{12}: 1-*S*&2-*U***PS*;
	$\bigcap_{i=1}^{3}\boldsymbol{G}_{\boldsymbol{F}\mathrm{N}i}^{\mathrm{II}}\left(R_r,\,R_p,R_y,\,0,\,0,\,0\right)$	N_{13}:3-*RRR*	N_{14}: 3-*UR*
Waist	$\boldsymbol{G}_{\boldsymbol{F}\mathrm{W}1}^{\mathrm{II}}\left(R_r,\,R_p,R_y,\,P_r,\,0,\,0\right)\cap\left(\bigcap_{i=2}^{4}\boldsymbol{G}_{\boldsymbol{F}\mathrm{W}i}^{\mathrm{I}}\left(P_{ri},\,P_{pi},\,P_{yi},\,R_{ri},\,R_{pi},\,R_{yi}\right)\right)$	W_{29}: 1-*SP*&3-*SPS*; W_{31}: 1-*URP*&3-*UPS*; W_{33}: 1-*RRRP*&3-*SRS*; W_{35}: 1-*RRRP*^{R}&3-*PU***S*; W_{37}: 1-*RR*$\hat{}$*U*&3-*PPPS*;	W_{30}: 1-*SP*&3-*PSS*; W_{32}: 1-*URP*&3-*PUS*; W_{34}: 1-*RRRP*&3-*RSS*; W_{36}: 1-*RRRPR*&3-*U***PS*; W_{38}: 1-*RR*$\hat{}$*U*&3-$P_aP_aP_aS$
	$\bigcap_{i=1}^{4}\boldsymbol{G}_{\boldsymbol{F}\mathrm{W}i}^{\mathrm{II}}\left(R_r,\,R_p,R_y,\,P_r,\,0,\,0\right)$	W_{39}: 4-*UPR*	W_{40}: 4-*RRRP*

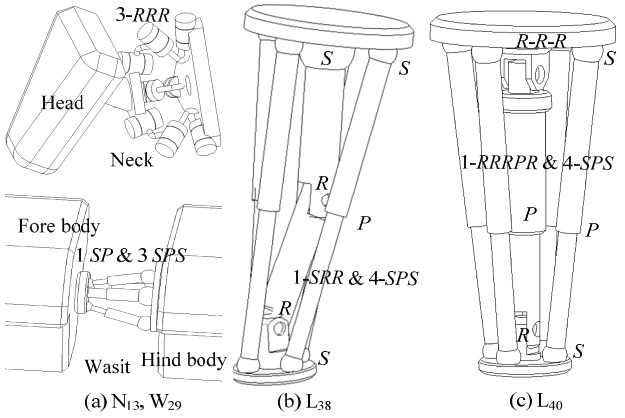

Fig. 7 Types of limbs with parallel topology.

ensure the irregular terrain adaptability. Fig. 8 shows the process from the biological type to serial types, and then to hybrid types. The kinematic chains in the brackets denote the parallel topology. Finally, 26 kinds of hybrid legs with 2-DOF parallel mechanism and 26 kinds of hybrid legs with 3-DOF parallel mechanism are produced (Table 4). Fig. 9 shows the examples of hybrid legs. It is easy to protect the hybrid legs from damage. For example, the actuations (like the motor) of the type L_{67} are centrally fixed on the body frame, as shown in Fig. 9d. For some specific quadruped robots, such as the rescue robot for nuclear accident, the electronic devices of the actuation can be easily fitted with lead shielding.

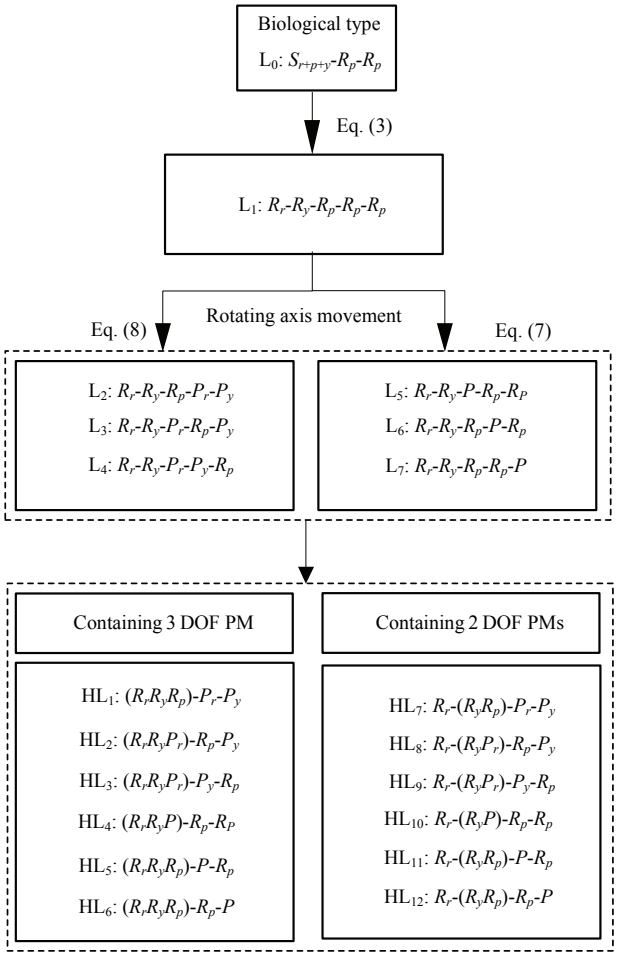

Fig. 8 Process of conversion from biological to hybrid types.

3.4 Types of quadruped robots

The type synthesis of quadruped robots was carried out in imitation of the biological types of quadruped mammals (Table 2). The generalized type equation of quadruped robots is N_i-W_j-L_k, where N_i, W_j and L_k denote the types of necks, waists, and legs (Table 5). Fig. 10 shows the examples of structures of quadruped robots. Some of the quadruped robots with serial and parallel topology have been used for the design of walking robots. For example, the neck and waist joints of N_1-W_1-L_{36} (Fig. 10b) of the quadruped robot are the RRR and RRRP serial configurations. Its legs consist of the *RR* kinematic chain, a composite kinematic pair U^P, and a revolute joint. The composite pair increases the stiffness of the serial leg. The neck, waist, and legs of N_{13}-W_{29}-L_{38} (Fig. 10c) all have parallel configurations, 3-*RRR*, 1-*SP*&3-*SPS* and 1-*SRRR*&4-*SPS* parallel mechanism, respectively. Recently, types of quadruped robots with hybrid legs have drawn considerable interest. Hybrid legs provide greater stiffness, can support larger payload, and are more agile than their serial and parallelcounterparts (Fig. 10d–10f). For example, the hybrid type N_1-W_1-L_{65} (Fig. 10d) is a typical configuration of a quadruped robot. This kind of leg has three active DOFs and two passive DOFs, which not only meets the motion requirement in 3D space but also has simplified leg structure. In addition, the actuations of this kind of hybrid legs are easily protected when their configurations change a little from *UP*&2-*SPS* to *PU*&2-*PSS* or *UP*&2-*UPS* to *PU*&*PUS* (Fig. 9d). The hybrid legs have been used for the design of rescue walking robots for nuclear accident response (Fig. 11). Fig. 11a shows the first generation of walking robots with the leg configurations of *UP*&2-*UPS*. In the second generation (Fig. 11b), the configuration of *PU*&2-*PUS* is used for the active part of the leg. In the meantime, a spatial four-bar mechanism is affixed to the end of the active mechanism to enlarge the workspace.

Table 4 Types of hybrid legs

No.	G_F sets of parallel parts	Example of type	
HL_1 HL_5 HL_6	$\boldsymbol{G}^{\mathrm{II}}_{FL1}(\mathrm{R}_{\alpha1},\mathrm{R}_{\beta1},\mathrm{R}_{\gamma1},0,0,0)\cap$ $\left(\bigcap_{i=2}^{3}\boldsymbol{G}^{\mathrm{I}}_{FLi}(\mathrm{P}_{ri},\mathrm{P}_{pi},\mathrm{P}_{yi},\mathrm{R}_{ri},\mathrm{R}_{pi},\mathrm{R}_{yi})\right)$	L_{50}: (*RRR*&2-*SPS*)-P_r-P_y; L_{52}: (*RRR*&2-*UPS*)-R_p-P; L_{54}: (*UR*&2-*RSS*)-P-R_p; L_{56}: (*RU*&2-PU^*S)-P_r-P_y; L_{58}: (*RU*&2-*PPPS*)-R_p-P;	L_{51}: (*RRR*&2-*PSS*)-P-R_p; L_{53}: (*UR*&2-*UPS*)-U_{r+p}; L_{55}: (*UR*&2-*SRS*)-R_p-P; L_{57}: (*RU*&2-U^*PS)-P-R_p; L_{59}: (*RRR*&2-$P_aP_aP_aS$)-P_r-P_y
	$\bigcap_{i=1}^{3}\boldsymbol{G}^{\mathrm{II}}_{FLi}(R_{\alpha i},R_{\beta i},R_{yi},0,0,0)$	L_{60}: (3-*RRR*)-P_r-P_y L_{62}: (3-*RU*)-R_p-P	L_{61}: (3-*UR*)-P-R_p
HL_2 HL_3 HL_4	$\boldsymbol{G}^{\mathrm{II}}_{FL1}(R_{\alpha1},R_{\beta1},P_i,0,0,0)\cap$ $\left(\bigcap_{i=2}^{3}\boldsymbol{G}^{\mathrm{I}}_{FLi}(P_{ri},P_{pi},P_{yi},R_{ri},R_{pi},R_{yi})\right)$	L_{63}: (*RRP*&2-*SPS*)-R_p-P_y; L_{65}: (*UP*&2-*SPS*)-U_{r+p}; L_{67}: (*PU*&2-*PUS*)-U_{r+p}; L_{69}: (*RRP* &2-PU^*S)-R_p-P_y; L_{71}: (*RRP*&2-*PPPS*)-U_{r+p};	L_{64}: (*RRP*&2-*PSS*)-P_y-R_p; L_{66}: (*UP*&2-*UPS*)-U_{r+p}; L_{68}: (*UP*&2-*SRS*)-R_p-R_r; L_{70}: (*RRP*&2-U^*PS)-P_y-R_p; L_{72}: (*UP*&2-$P_aP_aP_aS$)-R_p-P_y
	$\bigcap_{i=1}^{3}\boldsymbol{G}^{\mathrm{II}}_{FLi}(R_{\alpha i},R_{\beta i},P_i,0,0,0)$	L_{73}: (3-*RRP*)-R_p-P_y L_{75}: (3-*UP*)-R_p-R_P	L_{74}: (3-*RRP*)-P_y-R_p
HL_7 HL_{11} HL_{12}	$\boldsymbol{G}^{\mathrm{II}}_{FL1}(R_{\alpha1},R_{\beta1},0_1,0,0,0)\cap$ $\boldsymbol{G}^{\mathrm{I}}_{FL2}(P_{r2},P_{p2},P_{y2},R_{r2},R_{p2},R_{y2})$	L_{76}: R_r-(*RR*&*SPS*)-P_r-P_y; L_{78}: R_r-(*RR*&*UPS*)-U_{r+p}; L_{80}: R_r-(*U*&*SRS*)-P-R_p; L_{82}: R_r-(*RR*&PU^*S)-P_r-P_y; L_{84}: R_r-(*RR*&*PPPS*)-R_p-P;	L_{77}: R_r-(*RR*&*PSS*)-P-R_p; L_{79}: R_r-(*U*&*PUS*)-P_r-P_y; L_{81}: R_r-(*U*&*RSS*)-R_p-P; L_{83}: R_r-(*RR*&U^*PS)-P-R_p; L_{85}: R_r-(*U*&$P_aP_aP_aS$)-P_r-P_y
	$\bigcap_{i=1}^{2}\boldsymbol{G}^{\mathrm{II}}_{FLi}(R_{\alpha i},R_{\beta i},0,0,0,0)$	L_{86}: R_r-(2-*RR*)-P_r-P_y L_{88}: R_r-(2-*RR*)-R_p-P	L_{87}: R_r-(2-*RR*)-P-R_p
HL_8 HL_9 HL_{10}	$\boldsymbol{G}^{\mathrm{II}}_{FL1}(R_{\alpha1},P_1,0_1,0,0,0)\cap$ $\boldsymbol{G}^{\mathrm{I}}_{FL2}(P_{r2},P_{p2},P_{y2},R_{r2},R_{p2},R_{y2})$	L_{89}: R_r-(*RP*&*SPS*)-R_p-P_y; L_{91}: R_r-(*RP*&*SPS*)-U_{r+p}; L_{93}: R_r-(*RP* &*SRS*)-P_y-R_p; L_{95}: R_r-(*RP*&PU^*S)-R_p-P_y; L_{97}: R_r-(*RP*&*PPPS*)-R_r-R_P;	L_{90}: R_r-(*RP*&*PSS*)-P_y-R_p; L_{92}: R_r-(*RP*&*UPS*)-U_{r+p}; L_{94}: R_r-(*RP*&*RSS*)-R_r-R_P; L_{96}: R_r-(*RP*&U^*PS)-P_y-R_p; L_{98}: R_r-(*RP*&$P_aP_aP_aS$)-R_p-P_y
	$\bigcap_{i=1}^{2}\boldsymbol{G}^{\mathrm{II}}_{FLi}(R_{\alpha i},P_i,0,0,0,0)$	L_{99}: R_r-(2-*RP*)-R_p-P_y L_{101}: R_r-(2-*RP*)-R_p-R_P	L_{100}: R_r-(2-*RP*)-P_y-R_p

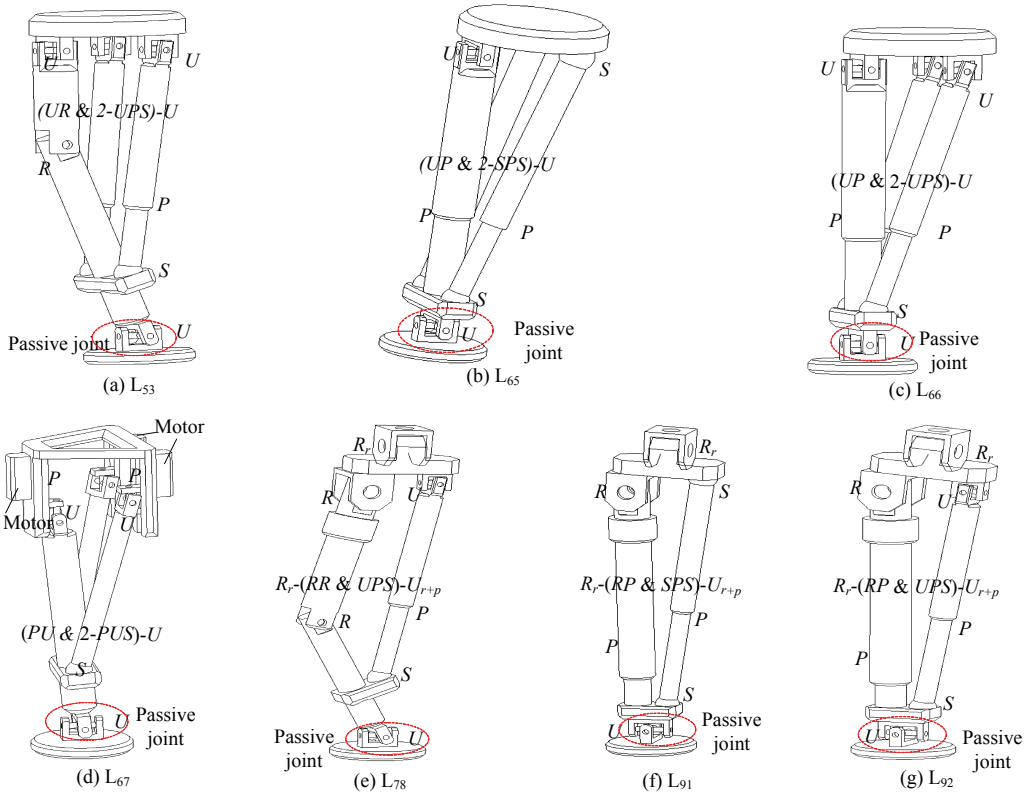

Fig. 9 Structures of legs with hybrid mechanism.

Table 5 Types of quadruped robots

Type	Conditions	Quantity	Examples
Serial topology	i = 0–4; j = 0–28; k = 0–37	5510	N_0-W_0-L_0, N_0-W_1-L_1, N_1-W_1-L_1, N_4-W_0-L_0, N_1-W_1-L_{36}…
Parallel topology	i = 5–14; j = 29–40; k = 38–49	1440	N_5-W_{29}-L_{38}, N_6-W_{29}-L_{38}, N_7-W_{29}-L_{38}, N_6-W_{30}-L_{39}, N_{13}-W_{29}-L_{38}…
Hybrid topology	i = 0–14; j = 0–40; k = 50–101	31980	N_1-W_1-L_{50}, N_2-W_2-L_{51}, N_2-W_3-L_{52}, N_1-W_1-L_{65}, N_{13}-W_1-L_{53}, N_4-W_0-L_{91}…

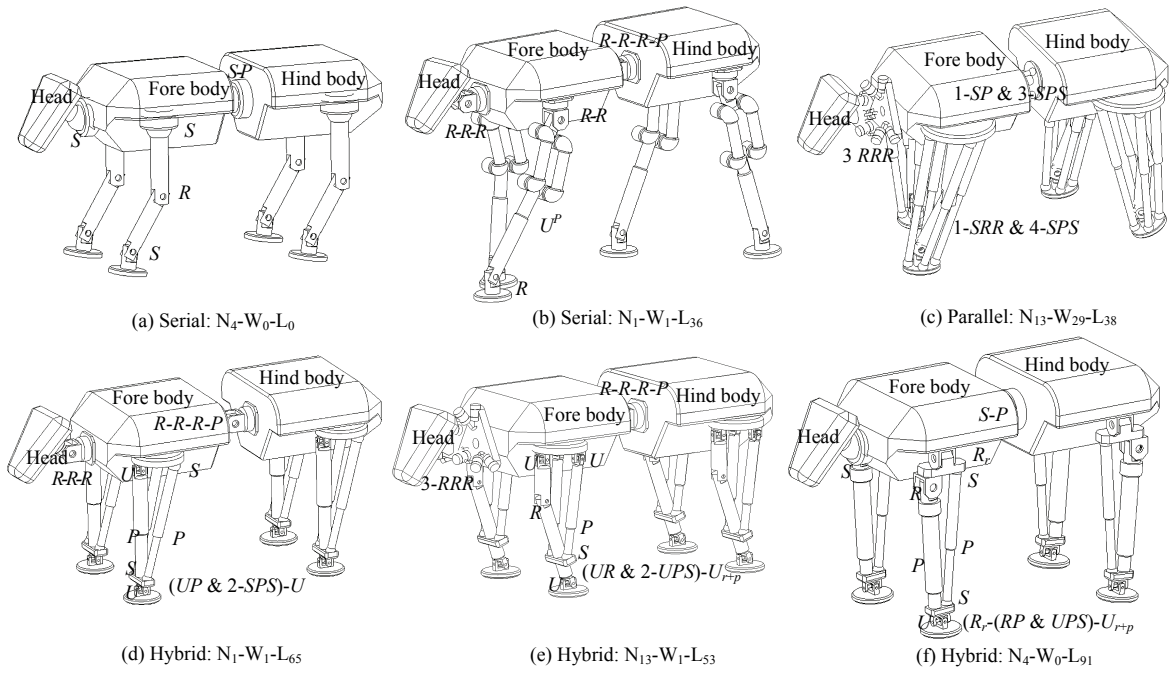

(a) Serial: N_4-W_0-L_0 (b) Serial: N_1-W_1-L_{36} (c) Parallel: N_{13}-W_{29}-L_{38}

(d) Hybrid: N_1-W_1-L_{65} (e) Hybrid: N_{13}-W_1-L_{53} (f) Hybrid: N_4-W_0-L_{91}

Fig. 10 Types of quadruped robots.

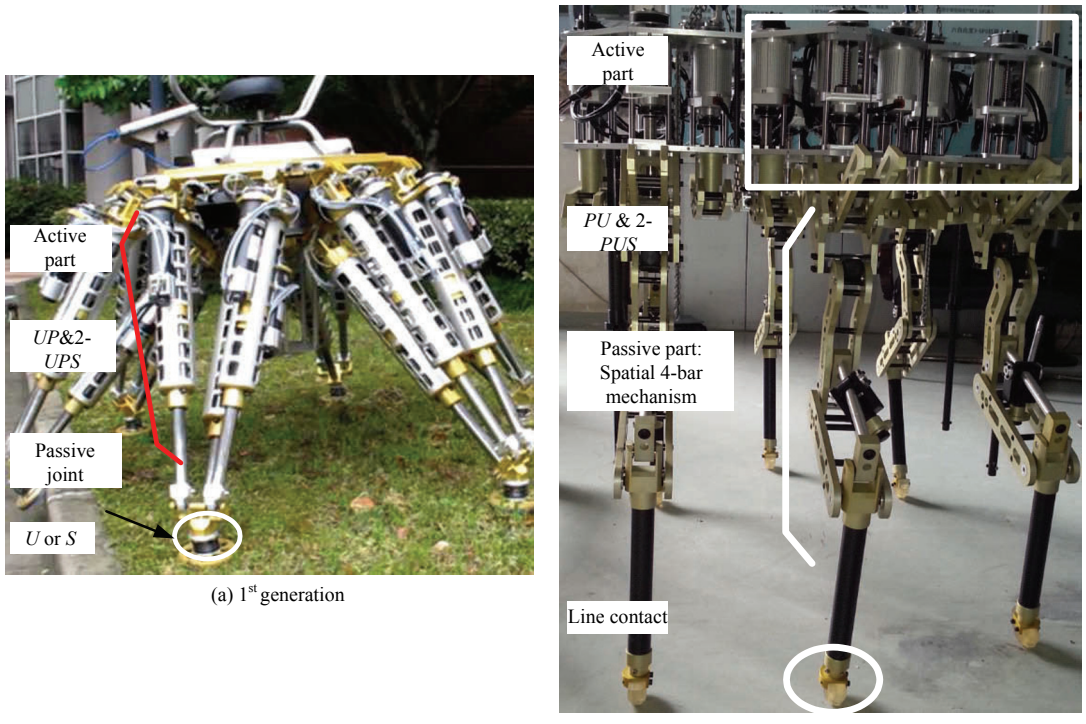

(a) 1st generation

(b) 2nd generation

Fig. 11 Rescue robots for nuclear accident.

4 Conclusion

A new approach to type synthesis for quadruped walking robots using biological types in serial, parallel, and hybrid formation based on the $\boldsymbol{G_F}$ set theory was proposed. The skeletal systems of quadruped mammals were analyzed. The patterns of motion of the cervical, thoracic, and lumbar vertebrae, all joints including the shoulder, elbow, carpal, hip, stifle, and tarsal joints were first presented using $\boldsymbol{G_F}$ sets. This showed that the $\boldsymbol{G_F}$ set theory can be applied to type synthesis of quadruped robots. The concept of type complexity is useful in simplifying the decomposition combinations of $\boldsymbol{G_F}$ sets.Then the process of type synthesis of quadruped robots from the biological type to serial, parallel, and hybrid types was proposed. Results showed that the axial movement and composite pair replacement were two effective means of producing new kinematic limbs. Finally, 37 kinds of serial legs, 4 kinds of serial necks, 28 kinds of serial waists, 12 kinds of parallel legs, necks, and waists, 26 kinds of hybrid legs with 2-DOF PM, and 26 kinds of hybrid legs with 3-DOF PM were produced, which provided references for the design of quadruped walking robots in the future. Six typical kinematic structures of quadruped robots with serial, parallel, and hybrid topology are presented as examples. Two of these configurations have been successfully used to design walking rescue robots suitable for responding to nuclear accidents.

Acknowledgment

This project is supported by National Basic Research Program of China (Grant No. 2013CB035501), National Natural Science Foundation of China (Grant No. 51205248), Shanghai Municipal Natural Science Foundation (Grant No. 12ZR1445200), Doctoral Programs Foundation of Ministry of Education of China (Grant No. 20120073120060).

References

[1] Guizzo E, Ackerman F. *Japanese Robot-SCHAFT*, [2013-4-10], http://spectrum.ieee.org/.

[2] Raibert M, Blankespoor K, Nelson G, Playter R. Bigdog: The rough-terrain quadruped robot. *Proceedings of the* 17*th World Congress of the International Federation of Automatic Control* (*IFAC*), USA, 2008, 71–82.

[3] Playter R, Buehler M, Raibert M. Bigdog. *Proceedings of the Society of Photo-optical Instrumentation Engineers* (*SPIE*), Orlando, USA, 2006, 6320.

[4] Kong X W, Gosselin C. *Type Synthesis of Parallel Mechanisms*, Springer, New York, 2007.

[5] Kong X W, Gosselin C. Type synthesis of 3-DOF translational parallel manipulators based on screw theory. *Journal of Mechanical Design*, 2004, **126**, 83–92.

[6] Kong X W, Gosselin C. Type synthesis of 3T1R 4-DOF parallel manipulators based on screw theory. *IEEE Transactions on Robotics and Automation*, 2004, **20**, 181–190.

[7] Kong X W, Gosselin C. Type synthesis of 3-DOF spherical parallel manipulators based on screw theory. *Journal of Mechanical Design*, 2004, **126**, 101–108.

[8] Huang Z, Li Q C. General methodology for type synthesis of lower-mobility symmetrical parallel manipulators and several novel manipulators. *International Journal of Robotics Research*, 2002, **21**, 131–145.

[9] Dai J S. An historical review of the theoretical development of rigid body displacements from Rodrigues parameters to the finite twist. *Mechanism and Machine Theory*, 2006, **41**, 41–52.

[10] Gogu G. Structural synthesis of fully-isotropic translational parallel robots via theory of linear transformations. *European Journal of Mechanics A*/*Solids*, 2004, **23**, 1021–1039.

[11] Yang T L, Jin Q, Liu X A. Structure synthesis of 4-DOF parallel robot mechanisms based on the units of single-opened-chain. *Proceedings of ASME Design Engineering Technical Conference and Computers and Information in Engineering Conference*, Pittsburgh, PA, 2001, DETC2001/DAC-21152.

[12] Xie F G, Li T M, Liu X J. Type synthesis of 4-DOF parallel kinematic mechanisms based on Grassmann line geometry and atlas method. *Chinese Journal of Mechanical Engineering*, 2013, **26**, 1073–1081.

[13] Fan C X, Liu H Z, Zhang Y B. Type synthesis of 2T2R, 1T2R and 2R parallel mechanisms. *Mechanism and Machine Theory*, 2013, **61**, 184–190.

[14] Herve J M. The Lie group of rigid body displacements, a fundamental tool for mechanism design. *Mechanism and Machine Theory*, 1999, **34**, 719–730.

[15] Meng J, Liu G F, Li Z X. A geometric theory for analysis and synthesis of sub-6 DOF parallel manipulators. *IEEE Transactions on Robotics*, 2007, **23**, 625–649.

[16] Gogu G. *Structural Synthesis of Parallel Robots*: *Part* 1: *Methodology*, Springer, New York, 2007.

[17] Gao F, Yang J L. *Topology Synthesis for Parallel Robotic Mechanisms*, CAS publications, Warsaw, 2013.

[18] Gao F, Yang J L, Ge J. Type synthesis of parallel mecha-

nisms having the second class GF sets and two dimensional rotations. *Journal of Mechanisms and Robotics*, 2011, **3**, 011003.

[19] Meng X D. *Fundamental Research on Type Synthesis Approach of Parallel Robotic Mechanism*. Doctoral thesis, Shanghai Jiao Tong University, China, 2015. (in Chinese)

[20] He J, Gao F, Meng X D, Guo W Z. Type synthesis for 4-DOF parallel press mechanism using GF set theory. *Chinese Journal of Mechanical Engineering*, 2015, **28**, 851–859.

[21] Yang J L, Gao F, Shi L F, Jin Z L. State classification for human hands. *Journal of Bionic Engineering*, 2008, **5**, 158–163.

[22] Miao Y J, Gao F, Pan D L. State classification and motion description for the lower extremity exoskeleton SJTU-EX. *Journal of Bionic Engineering* , 2014, **11**, 249–258.

[23] Yang J L, Gao F, Jin Z L, Shi L F. Classification of lying states for the humanoid robot SJTU-HR1. *Science in China Series E*: *Technological Sciences*, 2009, **52**, 1301–1311.

[24] Johnson A M, Koditschek D E. Toward a vocabulary of legged leaping. *Proceedings of the IEEE International Conference on Robotics and Automation*, Karlsruhe, Germany, 2013, 1–8.

[25] Eich M, Grimminger F, Kirchner F. A versatile stair-climbing robot for search and rescue applications. *Proceedings of the IEEE International Workshop on Safety*, *Security and Rescue Robotics*, Sendai, Japan, 2008, 35–40.

[26] Thomas A J, Roger Q D, Richard B J, Ritzmann R E. Abstracted biological principles applied with reduced actuation improve mobility of legged vehicles. *Proceedings of the IEEE/RSJ International Conference on Intelligent Robots and Systems*, Las Vegas, USA, 2003, 1370–1375.

[27] Cham J G, Bailey S A, Clark J E, Full R J, Cutkosky M R. Fast and robust: Hexapedal robots via shape deposition manufacturing. *The International Journal of Robotics Research*, 2002, **21**, 869–882.

[28] Poulakakis I, Papadopoulos E, Buehler M. On the stability of the passive dynamics of quadrupedal running with a bounding gait. *The International Journal of Robotics Research*, 2006, **25**, 669–87.

[29] Raibert M H, Chepponis M, Benjamin H J. Running on four legs as though they were one. *IEEE Journal of Robotics and Automation*. 1986, **2**, 70–82.

[30] De Santos P G, Garcia E, Cobano J, Ramirez A. SILO6: A six-legged robot for humanitarian de-mining tasks. *Proceedings of Automation Congress*, Seville, Spain, 2004, 523–528.

[31] Puch D R, Ribble E A, Vohnout V J, Bihari T E, Walliser T M, Patterson M R, Waldron K J. Technical description of the adaptive suspension vehicle. *The International Journal of Robotics Research*.1990, **9**, 24–42.

[32] Semini C, Tsagarakis N G, Guglielmino E, Focchi M, Cannella F, Caldwell D G. Design of HyQ-a hydraulically and electrically actuated quadruped robot. *Proceedings of the Institution of Mechanical Engineers* (*IMechE*), *Part I*: *Journal of Systems and Control Engineering*. 2011, **225**, 1–19.

[33] Galvez J A, Estremera J, Gonzalez S. A new legged-robot configuration for research in force distribution. *Mechatronics*, 2003, **13**, 907–932.

[34] Daud M R, Nonami K. Autonomous walking over obstacles by means of LRF for hexapod robot COMET-IV. *Journal of Robotics and Mechatronics*, 2012, **24**, 55–63.

[35] Chen X B, Gao F, Qi C K. Spring parameters design for the new hydraulic actuated quadruped robot. *Journal of Mechanism and Robotic*, 2014, **6**, 021003.

[36] Zhang J Q, Gao F, Han X L, Chen X B, Han X Y. Trot gait design and CPG method for a quadruped robot. *Journal of Bionic Engineering*, 2014, **11**, 18–25.

[37] Pan Y. *Performance Design and Control Experiment of a Novel Hexapod Robot with P-P Structure*, Doctoral thesis, Shanghai Jiao Tong University, China, 2014. (in Chinese)

[38] Henrey M, Ahmed A, Boscariol P, Shannon L, Menon C. Abigaille-III: A versatile, bioinspired hexapod for scaling smooth vertical surfaces. *Journal of Bionic Engineering*, 2014, **11**, 1–17.

[39] Chen J, Liu Y B, Zhao J, Zhang H, Jin H Z. Biomimetic design and optimal swing of a hexapod robot leg. *Journal of Bionic Engineering*, 2014, **11**, 26–35.

[40] Stephen Beck. *Skeletal System of a Dog*, [2015-5-13], http://oklahoma4h.okstate.edu/.

[41] Akers M R, Denbow D M. *Anatomy and Physiology of Domestic Animals*, 2nd ed, Wiley-Blackwell Press, New York, 2013.